JOURNAL OF GUIDANCE, CONTROL, AND DYNAMICS
Vol. 23, No. 5, September–October 2000

Periodic Solutions for Spinning Asymmetric Rigid Bodies with Constant Principal-Axis Torque

R. Anne Gick,* Marc H. Williams,† and James M. Longuski‡
Purdue University, West Lafayette, Indiana 47907-1282

We analyze the motion of a spinning asymmetric rigid body subject to constant torque along one of the principal axes. Periodic solutions for the angular velocity vector and the corresponding kinematic parameters are given in terms of Fourier series expansions. Three semi-analytic solution methods are presented: one-period integration, Newton's method, and a perturbation method. These are compared for computational efficiency with a given error bound. The solutions apply to arbitrarily large attitude motions. When multiple period solutions are desired, these methods always prove more efficient than straightforward numerical integration. The techniques may be applied to onboard computations, maneuver analysis, and maneuver optimization.

Introduction

THE motion of a rigid body subjected to body-fixed torques, where the moments of inertia do not change appreciably, is known as the self-excited rigid-body problem. This problem was first clearly defined by Grammel (see Ref. 1) and has occupied a number of investigators over the past few decades.[1–9] Leimanis[1] gives an excellent account of the (largely academic) literature up until the mid-1960s. With the advent of the space program, researchers have looked at the self-excited rigid body with new interest because it is highly relevant to spacecraft. Variations on this theme include analysis of the motion of axisymmetric, near-symmetric, and asymmetric rigid bodies, subject to constant and time-varying body-fixed torques, during small- and large-angle excursions of the spin axis. In general the problem is intractable with respect to the goal of finding closed-form, exact analytic solutions, and each author has been forced to make concessions in simplifying the analysis to fit the exigencies of the particular application.

In this paper we address the problem of characterizing the full (dynamics and kinematics) motion of a spinning asymmetric rigid body with constant torque on a principal axis when the motion is periodic. In general, when a constant body-fixed torque is applied to a spinning rigid body, the resulting motion is either a progressive spinup to high angular velocity or a bounded oscillation, depending on the initial angular velocity and on the magnitude and orientation of the applied torque. Our previous work[10] on this problem was restricted to a spinning axisymmetric body with transverse torque. In this case the spin about the major axis remains constant, while the transverse spins undergo a simple harmonic variation. The attitude motion is, therefore, amenable to Fourier–Floquet techniques.[11,12] When these techniques are applied to a nearly axisymmetric body, the results are excellent for small torque, but the errors increase with increasing torque. In the present paper we generalize to an arbitrary asymmetric body, and proceed to use Fourier-Floquet methods to analyze the spin and attitude motions for all cases where the angular velocity is oscillatory. (For other dynamics applications of Floquet theory see Calico and Wiesel,[13] Mingori,[14] and Noah and Hopkins.[15])

The dynamical solutions are discussed in detail in the work of Livneh and Wie,[16] though without addressing the kinematics. We borrow certain of their results here, repeating only as much as necessary for clarity. The essential result is that the angular velocity vector can be periodic only if the applied torque is perfectly aligned with one of the three principal axes. Any misalignment will cause the body to spinup (though for small misalignments, the process takes a long time). The periodic solutions can be divided into two classes: 1) torque along the major or minor (stable) axis and 2) torque along the intermediate (unstable) axis. In the first case, the resulting motion will be periodic only for certain initial conditions and torque magnitudes. In the second case, the motion will be periodic for (essentially) any initial condition and torque magnitude. Our goal is to describe efficient, that is, semi-analytical, methods for computing the angular velocity and attitude for all cases where the motion is periodic. Three methods are presented and compared.

Received 19 August 1999; revision received 24 February 2000; accepted for publication 24 February 2000.

*Doctoral Candidate, School of Aeronautics and Astronautics. Formerly R. Anne Beck. Student Member AIAA.

†Professor and Associate Head, School of Aeronautics and Astronautics. Member AIAA.

‡Professor, School of Aeronautics and Astronautics. Associate Fellow AIAA.

Euler's Equations of Motion

We begin our analysis for the attitude motion of a rigid body by considering Euler's equations of motion:

$$I_x\dot{\omega}_x = M_x - (I_z - I_y)\omega_y\omega_z \tag{1}$$

$$I_y\dot{\omega}_y = M_y - (I_x - I_z)\omega_z\omega_x \tag{2}$$

$$I_z\dot{\omega}_z = M_z - (I_y - I_x)\omega_x\omega_y \tag{3}$$

where M_x, M_y, and M_z are torque components; ω_x, ω_y, and ω_z are angular velocity components; and I_x, I_y, and I_z are principal moments of inertia. Without loss of generality, we also assume that I_y is the intermediate principal moment of inertia

$$I_{\min} < I_y < I_{\max} \tag{4}$$

We can rewrite Euler's equations (1–3) in the following nondimensional form[16]:

$$\frac{\mathrm{d}X}{\mathrm{d}T} = -YZ + \mu_x \tag{5}$$

$$\frac{\mathrm{d}Y}{\mathrm{d}T} = ZX + \mu_y \tag{6}$$

$$\frac{\mathrm{d}Z}{\mathrm{d}T} = -XY + \mu_z \tag{7}$$

by introducing the following time and amplitude scaling parameters

$$T = ht \tag{8}$$

$$X = \omega_x/(h\kappa_x), \qquad Y = \omega_y/(h\kappa_y), \qquad Z = \omega_z/(h\kappa_z) \tag{9}$$

and

$$\mu_x = M_x\Big/\left(h^2 I_x\kappa_x\right), \qquad \mu_y = M_y\Big/\left(h^2 I_y\kappa_y\right)$$

$$\mu_z = M_z\Big/\left(h^2 I_z\kappa_z\right) \tag{10}$$

The nondimensional inertia parameters, κ_x, κ_y, and κ_z, are given by

$$\kappa_x^2 = \frac{I_y I_z}{(I_z - I_x)(I_y - I_x)}, \qquad \kappa_y^2 = \frac{I_z I_x}{(I_z - I_y)(I_y - I_x)}$$

$$\kappa_z^2 = \frac{I_x I_y}{(I_z - I_x)(I_z - I_y)} \tag{11}$$

These parameters are not independent, but are related by

$$\kappa_x^2 - \kappa_y^2 + \kappa_z^2 = 1 \tag{12}$$

If the torque is constant, we can choose the frequency scale h as follows:

$$h = \left\{ \left[M_x/(I_x \kappa_x) \right]^2 + \left[M_y/(I_y \kappa_y) \right]^2 + \left[M_z/(I_z \kappa_z) \right]^2 \right\}^{\frac{1}{4}} \tag{13}$$

so that μ_x, μ_y, and μ_z, form the components of a unit vector

$$\mu_x^2 + \mu_y^2 + \mu_z^2 = 1 \tag{14}$$

We are particularly interested in those situations in which the solution of Eqs. (5–7) are periodic. This can happen only if the applied torque is aligned with one of the principal axes.[16] There are three cases to be studied:

$$\boldsymbol{\theta} = \begin{bmatrix} \mu_x \\ \mu_y \\ \mu_z \end{bmatrix} = \begin{bmatrix} 1 \\ 0 \\ 0 \end{bmatrix}, \begin{bmatrix} 0 \\ 1 \\ 0 \end{bmatrix}, \begin{bmatrix} 0 \\ 0 \\ 1 \end{bmatrix} \tag{15}$$

However, because Eqs. (5–7) are symmetric in the interchange of X and Z, only the first two need be examined. When $\boldsymbol{\theta} = [0, 1, 0]$, Eqs. (5–7) have equilibrium points at $XZ = -1$ and $Y = 0$ with similar results for the other two cases. The stability characteristics of these equilibrium points have been discussed in Ref. 16.

The nearly symmetric case, studied in Ref. 10, for which

$$\kappa_x \approx \kappa_y \gg 1, \qquad \kappa_z \approx 1 \tag{16}$$

corresponds to the limit of infinitesimal X, Y. In that limit (when $\mu_z = 0$), Z remains nearly constant while X and Y undergo a simple harmonic variation with frequency Z. Evidently this solution applies whenever X and Y are much less than Z, whatever the reason (near symmetry, large z spin, or small torque). In the general case, Eqs. (5–7) are reducible to quadrature when the torque is aligned [Eq. (15)].

Constant Torque Along the Intermediate Axis

When the torque is applied along the intermediate, or unstable axis, $\boldsymbol{\theta} = [0, 1, 0]^T$, the rigid-body motion described by Eqs. (5–7) is equivalent to the motion of a particle moving in a one-dimensional potential well. To demonstrate this, we introduce a new variable $\theta(T) = -2 \tanh^{-1}(X/Z)$, so that the angular velocities can be written as

$$X = -R \sinh(\theta/2) \tag{17}$$

$$Y = \frac{1}{2} \frac{\mathrm{d}\theta}{\mathrm{d}T} \tag{18}$$

$$Z = R \cosh(\theta/2) \tag{19}$$

where $R = \sqrt{(Z^2 - X^2)}$ is constant. Because R is constant, then when θ is periodic X, Y, and Z will also be periodic. Note that because the equation pair (5) and (7) is invariant under the interchange of X and Z, we may assume $|Z| \geq |X|$. Moreover, because these equations are also symmetric under the interchange of X with $-X$ and Z with $-Z$, we may always arrange for $Z > 0$, so that R and θ are real. From these definitions and Eqs. (5–7), we obtain a single second-order equation

$$\frac{\mathrm{d}^2\theta}{\mathrm{d}T^2} + R^2 \sinh\theta = 2 \tag{20}$$

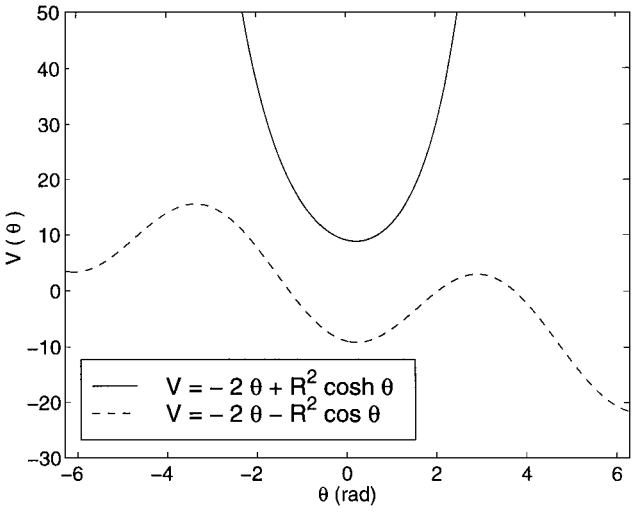

Fig. 1 Potential well characterization, $R = 3$.

which is the equation of motion of a particle moving in a potential well:

$$V(\theta) = -2\theta + R^2 \cosh\theta \tag{21}$$

where the corresponding energy integral is

$$E = X^2 + Y^2 - \theta \tag{22}$$

(Note that with these definitions, kinetic energy is $2E - V$.) This potential energy is plotted in Fig. 1 for the special case $R = 3$ (solid line). Because $V(\theta)$ is strictly convex, θ will necessarily oscillate between two extreme values that depend on the total energy E. The potential is convex regardless of the value of R (provided $R \neq 0$), so all motion in this class will be periodic, regardless of the initial conditions. The only exception is when $X = Z$ initially. In this case ($R = 0$), the asymptotic behavior is spinup, $X = Z \to 0$, $\mathrm{d}Y/\mathrm{d}T \to 1$; although this solution is structurally unstable. In contrast, when $X = -Z$ initially (so $R = 0$), the motion is periodic.

Constant Torque Along the Minor (Major) Axis

When the torque is applied along either of the two stable principal axes, $\boldsymbol{\theta} = [1, 0, 0]^T$ or $[0, 0, 1]^T$, the Euler equations (5–7) can be represented by a similar, but qualitatively different, physical equivalent. We introduce a new variable $\theta(T) = 2 \tan^{-1}(Y/Z)$, from which the angular velocities are determined, for $\boldsymbol{\theta} = [1, 0, 0]^T$:

$$X = \frac{1}{2} \frac{\mathrm{d}\theta}{\mathrm{d}T} \tag{23}$$

$$Y = R \sin(\theta/2) \tag{24}$$

$$Z = R \cos(\theta/2) \tag{25}$$

where $R = \sqrt{(Y^2 + Z^2)}$ is constant. Because R is constant, then when θ is periodic X, Y, and Z will also be periodic. (The case for $\boldsymbol{\theta} = [0, 0, 1]^T$ is trivially determined by interchanging X and Z.) With this substitution, the Euler equations reduce to

$$\frac{\mathrm{d}^2\theta}{\mathrm{d}s^2} + \sin\theta = \frac{2}{R^2} \tag{26}$$

where $s = R\,T$. This is equivalent to a particle moving in a one-dimensional potential well:

$$V(\theta) = -2\theta - R^2 \cos\theta \tag{27}$$

which is shown by the dashed line in Fig. 1 for $R = 3$. The corresponding energy integral is given by Eq. (22).

It is apparent from Fig. 1 that the potential well now has finite depth, so that the oscillations occur only for a range of energies E bounded by the extrema of V. When the energy is outside this range, the body will spin up along the x axis.

In this case, the rigid-body angular velocity motion is analogous to the motion of a forced simple pendulum. The equation of motion for a simple pendulum[17] of length l and mass m with a transversely applied constant force is given by

$$\frac{d^2\theta}{ds^2} + \sin\theta = \frac{F}{mg} \tag{28}$$

where $s = t\sqrt{(g/l)}$ and $F/(mg)$ is the thrust-to-weight ratio.

We note that if the thrust-to-weight ratio is greater than one, the pendulum will rotate. When the ratio is less than or equal to one, the pendulum will either rotate or oscillate depending on the initial energy. Analogously, the rigid body spins up if the ratio $2/R^2$ is greater than one. When $2/R^2$ is less than or equal to one, the rigid body will either spin up or oscillate about the equilibrium point $\theta = \sin^{-1}(2/R^2)$, depending on the initial energy.

The boundary between periodic motion and spinup can be determined by computing the largest energy E consistent with being inside the potential well (Fig. 1). The range of energies for which periodic motion occurs is $E^- \leq E \leq E^+$, where

$$E^{\pm} = R^2/2 - \pi/2 \pm \left[\sqrt{R^4/4 - 1} + \sin^{-1}(2/R^2) - \pi/2\right] \tag{29}$$

(with the arcsine taken to lie in the principal branch $[0, \pi/2]$). This domain is shown in Fig. 2. (The × and ○ indicate the test cases of Fig. 3 where $M_x = 200$ N · m and $M_x = 10$ N · m, respectively.) Near the lower energy limit, the body executes small-amplitude harmonic oscillations about the equilibrium point. At the upper energy limit, the body executes a large-, but finite, amplitude oscillation

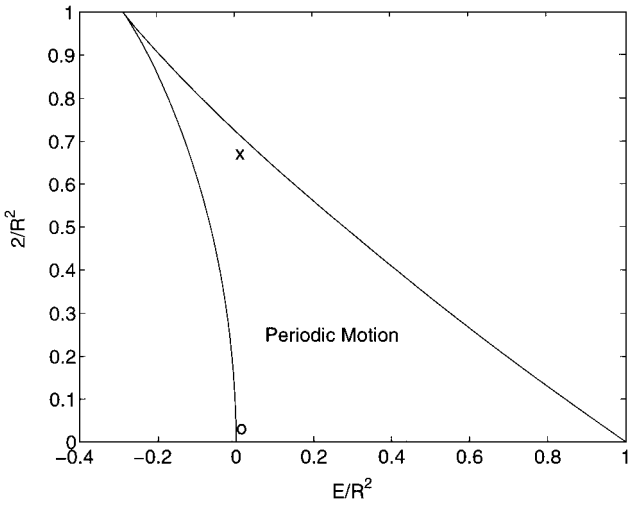

Fig. 2 Bounded periodic motion space for minor-axis torque.

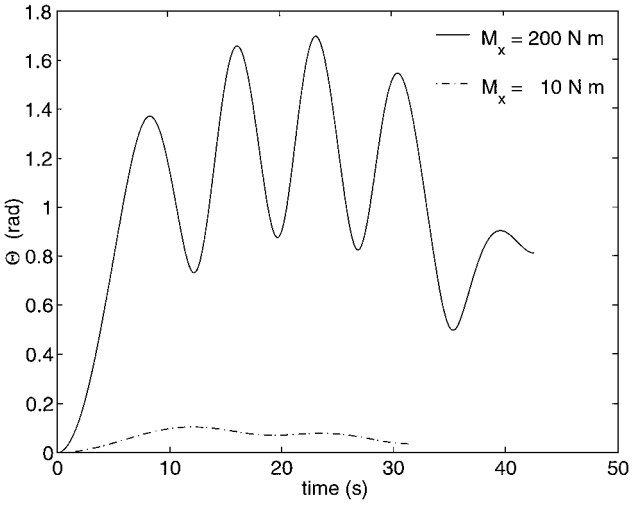

Fig. 3 Nutation angle $\Theta(t)$ for $M_x = [10, 200]$ N · m.

with infinite period. The two bounds coalesce at $R^2 = 2$ (where $E^{\pm} = 1 - \pi/2$), which is the equilibrium point $X = 0$, $Y = Z = 1$. In the pendulum analogy, this point corresponds to the mass lying in the horizontal position supported by the thrust, an obviously critical configuration on the verge of either rotation or oscillation, depending on how it is perturbed.

Reference 16 presents a three-dimensional surface representation of the periodic boundary in the XYZ state space. Whereas the present two-dimensional result of Eq. (29) and Fig. 2 is less intuitive, it is more compact and allows a simple test for periodicity of given initial conditions (because E and R are completely determined by the initial conditions on X, Y, and Z).

Determination of Period

When the angular velocity motion is periodic, the corresponding nondimensional period $\tilde{\mathcal{P}}$ is given by

$$\tilde{\mathcal{P}} = \int_{\theta_{\min}}^{\theta_{\max}} \frac{d\theta}{\sqrt{E + \theta - R^2\,\sigma(\theta)}} \tag{30}$$

where

$$\sigma(\theta) = \begin{cases} \sin^2(\theta/2) & \text{major or minor axis torque} \\ \sinh^2(\theta/2) & \text{intermediate axis torque} \end{cases} \tag{31}$$

The turning points, $\theta_{\min}$ and $\theta_{\max}$, are the zeros of the radicand. We evaluate this integral numerically because there is no closed-form solution for it. However, because the integrand is infinite at the endpoints, we employ a cosine transformation:

$$\theta(\xi) = [(\theta_{\min} + \theta_{\max})/2] + [(\theta_{\min} - \theta_{\max})/2]\cos\xi \tag{32}$$

to regularize the integral. This leads to

$$\tilde{\mathcal{P}} = \left(\frac{\theta_{\max} - \theta_{\min}}{2}\right)\int_0^{\pi} \frac{\sin\xi}{\sqrt{E + \theta(\xi) - R^2\sigma[\theta(\xi)]}}\,d\xi \tag{33}$$

With this transformation, the period integral can be numerically computed to any desired accuracy. When $\theta_{\max} - \theta_{\min}$ is small, the integral can be approximated by

$$\tilde{\mathcal{P}} = 2\pi/(R^4 \pm 4)^{\frac{1}{4}} \tag{34}$$

where the + and − correspond to the intermediate-axis and minor-axis cases, respectively.

The corresponding nondimensional frequency is given by

$$\tilde{\nu} = 2\pi/\tilde{\mathcal{P}} \tag{35}$$

Using the time transformation given in Eq. (8), we denote the values for dimensional period and frequency as $\mathcal{P} = \tilde{\mathcal{P}}/h$ and $\nu = h\tilde{\nu}$, respectively.

If we replace $\theta_{\max}$ in Eq. (30) with θ (varying from $\theta_{\min}$ to $\theta_{\max}$), the integral gives twice the nondimensional time $2T$, thereby implicitly defining the solution $\theta(T)$ over a half-period. The solution over the full period is obtained by reflection. This solution by quadrature has not been used in the present work, although it is a feasible alternative.

Kinematic Equations

The body orientation can be described using Cayley–Klein parameters (see Refs. 18 and 19) $[\alpha, \beta]$. These parameters are complex, but satisfy a normalization $|\alpha|^2 + |\beta|^2 = 1$, so that they contain only three degrees of freedom. The transformation between a body position $P = [x, y, z]^T$ and its inertial space image $P' = [x', y', z']^T$ can be expressed by $P' = RP$, where

$$R = \text{real}\begin{bmatrix} \alpha^2 - \beta^2 & i(\alpha^2 + \beta^2) & 2\alpha\beta \\ -i(\alpha^2 - \beta^2) & \alpha^2 + \beta^2 & -2i\alpha\beta \\ -2\alpha\bar{\beta} & -2i\alpha\bar{\beta} & |\alpha|^2 - |\beta|^2 \end{bmatrix} \tag{36}$$

with complex conjugation denoted by overbars. Clearly this rotation matrix is quadratic in $[\alpha, \beta]$ and reduces to the identity matrix

when $\alpha = 1$, $\beta = 0$. For example, a fixed point on the major axis, $P = [0, 0, 1]^T$, will move along an inertial space trajectory

$$x' + iy' = 2\alpha\beta, \qquad z' = |\alpha|^2 - |\beta|^2 \tag{37}$$

From this we see that the angle between the z and z' axes, or nutation,[20] is

$$\Theta = 2\cos^{-1}(|\alpha|) \tag{38}$$

whereas the precession angle is

$$\phi = \angle(\alpha\beta) \tag{39}$$

Similarly, any of the other commonly used Eulerian angle parameterizations can be expressed in terms of $[\alpha, \beta]$. The relations with the 3–2–1 sequence is given in Ref. 10.

The reason for adopting the Cayley–Klein parameterizationis that $[\alpha, \beta]$ obey linear homogeneous differential equations (in strong contrast to Eulerian angles):

$$\dot{\alpha} = (i\omega_z/2)\alpha - (i\bar{\omega}/2)\beta \tag{40}$$

$$\dot{\beta} = -(i\omega/2)\alpha - (i\omega_z/2)\beta \tag{41}$$

where

$$\omega = \omega_x + i\omega_y \tag{42}$$

These equations have a general invariant $|\alpha|^2 + |\beta|^2$, which, as already noted, is taken to be 1 by definition.

We have shown that the dimensional Euler's equations (1–3) can be reduced by scaling to a parameterless form [Eqs. (5–7)]. The same scaling applied to the kinematic equations (40) and (41) yields

$$\frac{d\alpha}{dT} = \frac{i}{2}[\kappa_z Z\alpha - \bar{\Omega}\beta] \tag{43}$$

$$\frac{d\beta}{dT} = -\frac{i}{2}[\Omega\alpha + \kappa_z Z\beta] \tag{44}$$

where $\Omega = \kappa_x X + i\kappa_y Y$. Therefore, the eccentricities of the body, as measured by the κs, affect the orientation, even though they have no effect on the scaled dynamics.

When the angular velocities vary periodically in time, the Cayley–Klein parameters vary quasi periodically. Therefore, the kinematic problem can be solved using Fourier–Floquet methods, as in our earlier work[10] on axisymmetric bodies. The essential idea is that there must exist a solution of Eqs. (40) and (41), $[\alpha_q, \beta_q]$, of the form

$$\alpha_q = e^{-ist}u(t) \tag{45}$$

$$\beta_q = e^{-ist}v(t) \tag{46}$$

where $[u, v]$ are periodic with period $\mathcal{P}$ and s is a constant to be determined. Once such a solution has been found, the general solution can be constructed:

$$\alpha = C_1\alpha_q + C_2\bar{\beta}_q \tag{47}$$

$$\beta = C_1\beta_q - C_2\bar{\alpha}_q \tag{48}$$

where $[C_1, C_2]$ are free constants that can be used to match any initial conditions. To make use of this general solution, we need efficient ways to determine the periodic functions $[u, v]$ and the parameter s. We will present three such methods.

One-Period Numerical Integration

When the angular velocities are periodic, the Cayley–Klein parameters are quasi periodic, which means they never repeat. Nevertheless, the general form of these parameters, for arbitrary time and arbitrary initial conditions, can be deduced from one particular solution over one period of the angular velocities.

Let $[\alpha_1, \beta_1]$ be the particular solution of Eqs. (40) and (41) with initial conditions $[1, 0]$ at $t = 0$. This solution can be obtained from a numerical integration over one period $0 \le t \le \mathcal{P}$. From the symmetries of Eqs. (40) and (41), the general solution for any initial conditions $[\alpha(0), \beta(0)]$ must be

$$\alpha = \alpha(0)\alpha_1(t) - \beta(0)\bar{\beta}_1(t) \tag{49}$$

$$\beta = \alpha(0)\beta_1(t) + \beta(0)\bar{\alpha}_1(t) \tag{50}$$

However, because $[\alpha_1, \beta_1]$ have been determined only over one period, we need to continue this solution into $t > \mathcal{P}$ to have the solution for all time.

Let $[\alpha_{q0}, \beta_{q0}]$ be the initial conditions required to produce a solution of the form shown in Eqs. (45) and (46). Then the conditions that u and v repeat at the end of one period provide

$$\cos(s\mathcal{P}) = \text{real}[\alpha_1(\mathcal{P})] \tag{51}$$

$$\alpha_{q0} = K\bar{\beta}_1(\mathcal{P}) \tag{52}$$

$$\beta_{q0} = K\left(\alpha_1(\mathcal{P}) - e^{-is\mathcal{P}}\right) \tag{53}$$

where K is an arbitrary normalization factor. It makes no difference which of the infinite number of s values satisfying Eq. (51) is chosen because different choices amount to redefinitions of the $[u, v]$, with no change in $[\alpha, \beta]$. It follows immediately that the periodic functions $[u, v]$ are

$$u = e^{ist}[\alpha_{q0}\alpha_1 - \beta_{q0}\bar{\beta}_1] \tag{54}$$

$$v = e^{ist}[\alpha_{q0}\beta_1 + \beta_{q0}\bar{\alpha}_1] \tag{55}$$

which define $[u, v]$ for all t because they are periodic.

Finally, the fundamental solution $[\alpha_1, \beta_1]$ can be continued to all t using

$$\alpha_1 = -\bar{\alpha}_{q0}e^{-ist}u + \beta_{q0}e^{ist}\bar{v} \tag{56}$$

$$\beta_1 = \bar{\alpha}_{q0}e^{-ist}v - \beta_{q0}e^{ist}\bar{u} \tag{57}$$

where we have assumed a normalization $|\alpha_{q0}|^2 + |\beta_{q0}|^2 = 1$. The solution for arbitrary initial conditions and arbitrary time can now be evaluated from Eqs. (49) and (50).

Fourier–Floquet Techniques

Because the angular velocities and kinematic parameters $[u, v]$ are periodic, we can express them using Fourier series as follows:

$$[X \;\; Y \;\; Z \;\; u \;\; v] = \sum_{n=-\infty}^{\infty} [X_n \;\; Y_n \;\; Z_n \;\; u_n \;\; v_n]E_n \tag{58}$$

where X_n, Y_n, Z_n, u_n, and v_n are the Fourier coefficients and E_n is the complex sinusoid:

$$E_n = e^{in\tilde{\nu}T} = e^{in\nu t} \tag{59}$$

One straightforward way of determining the Fourier coefficients is by performing a Fast Fourier Transform (FFT) analysis of the discrete time histories obtained from one-period numerical integration. The main advantage is that the algorithm is stored compactly because relatively few coefficients must be retained.

However, the governing differential equations (5–7) and (40) and (41), contain no more than products of periodic functions, so that a purely algebraic attack on the Fourier coefficients is feasible. Substituting the Fourier series, Eq. (58), into the nondimensional Euler's equations (5–7), and equating the coefficients of E_n, we find that the coefficients of the angular velocities must obey

$$in\tilde{\nu}X_n + \sum_{m=-\infty}^{\infty} Y_{n-m}Z_m - \mu_x\delta_{n0} = 0 \tag{60}$$

$$in\tilde{\nu}Y_n - \sum_{m=-\infty}^{\infty} Z_{n-m}X_m - \mu_y\delta_{n0} = 0 \tag{61}$$

$$in\tilde{\nu}Z_n + \sum_{m=-\infty}^{\infty} X_{n-m}Y_m - \mu_z\delta_{n0} = 0 \tag{62}$$

where δ_{n0} is the Kronecker delta. To complete the set we also need to enforce specified initial conditions

$$\sum_{n=-\infty}^{\infty} [X_n \;\; Y_n \;\; Z_n] = [X(0) \;\; Y(0) \;\; Z(0)] \tag{63}$$

This set of nonlinear infinite-dimensional equations (60–63) must be solved for the coefficients $[X_n, Y_n, Z_n]$ and the frequency $\tilde{\nu}$.

Similarly, algebraic constraints on the kinematic solution can be obtained by substituting Eqs. (45), (46), and (58) into Eqs. (40) and (41):

$$(s + n\nu)u_n = \frac{1}{2}\sum_{m=-\infty}^{\infty} (\omega_{zm} u_{n-m} - \bar{\omega}_{-m} v_{n-m}) \tag{64}$$

$$(s + n\nu)v_n = -\frac{1}{2}\sum_{m=-\infty}^{\infty} (\omega_m u_{n-m} + \omega_{zm} v_{n-m}) \tag{65}$$

where $\nu = h\tilde{\nu}$ and $\omega_{xn} = h\kappa_x X_n$, etc., are considered known. These (infinite-dimensional) linear equations are homogeneous in $[u_n, v_n]$ and can be solved with a normalization constraint $u_0 = 1$. Once a solution is found, for $[u_n, v_n]$ and s, it can be renormalized to $|u|^2 + |v|^2 = 1$.

We investigate two methods (a Newton iteration and a perturbation expansion) for solving both the dynamics problem (60–63) and the kinematics problem (64) and (65). In both procedures the series are truncated by neglecting all terms with $|n| > N$. The retained $(2N + 1)$ coefficients are then estimated, by either Newton iteration or perturbation. If any of the tail coefficients, $n = \pm N$, exceed the error bound, then N is increased by 1 for the next iteration. The iteration stops when the largest change in any coefficient is smaller than the error bound. We usually begin with $N = 1$, unless a better initial guess is available. This ensures that the series will be no longer than necessary to achieve the specified accuracy.

Newton's Method

For any given truncation level N, the algebraic equations can be expressed compactly as $\boldsymbol{F}(\boldsymbol{U}) = 0$, where $\boldsymbol{U}$ is a state vector containing both the Fourier coefficients and the unknown frequency ($\tilde{\nu}$ or s). To implement a Newton iteration we need only define $\boldsymbol{U}$, $\boldsymbol{F}$, the Jacobian $\mathrm{d}\boldsymbol{F}/\mathrm{d}\boldsymbol{U}$, and an initial guess for $\boldsymbol{U}$.

For the dynamics problem [Eqs. (60–63)], we take $\boldsymbol{U}$ to be the column vector

$$\boldsymbol{U} = [\boldsymbol{X}^T \quad \boldsymbol{Y}^T \quad \boldsymbol{Z}^T \quad \tilde{\nu}]^T \tag{66}$$

where $\boldsymbol{X}$, $\boldsymbol{Y}$, and $\boldsymbol{Z}$ denote column vectors obtained by stacking the $(2N + 1)$ Fourier coefficients X_n, Y_n, and Z_n, for example,

$$\boldsymbol{X} = [X_{-N} \quad X_{-N+1} \quad \cdots \quad X_{-2} \quad X_{-1} \quad X_0 \quad X_1 \quad X_2 \quad \cdots \quad X_N]^T \tag{67}$$

The equations, then, are

$$\boldsymbol{F}(\boldsymbol{U}) = \begin{bmatrix} i\tilde{\nu}[n]\boldsymbol{X} + \hat{Y}\boldsymbol{Z} - \mu_x\boldsymbol{\delta} \\ i\tilde{\nu}[n]\boldsymbol{Y} - \hat{Z}\boldsymbol{X} - \mu_y\boldsymbol{\delta} \\ i\tilde{\nu}[n]\boldsymbol{Z} + \hat{X}\boldsymbol{Y} - \mu_z\boldsymbol{\delta} \\ \sum_n X_n - X(0) \\ \sum_n Y_n - Y(0) \\ \sum_n Z_n - Z(0) \end{bmatrix} \tag{68}$$

where

$$[n] = \mathrm{diag}(-N, \ldots, -2, -1, 0, 1, 2, \ldots, N) \tag{69}$$

$$\boldsymbol{\delta} = [\ldots, 0, 1, 0, \ldots]^T \tag{70}$$

and the matrices denoted by the caret (^) have Toeplitz structure, for example,

$$\hat{X} = \begin{bmatrix} X_0 & X_{-1} & X_{-2} & \cdots \\ X_1 & X_0 & X_{-1} & \\ X_2 & X_1 & X_0 & \\ \vdots & & & \ddots \end{bmatrix} \tag{71}$$

This matrix is padded with zeros in the upper right and lower left corners to make $\hat{X}(2N + 1)$ square.

The Jacobian can readily be computed

$$\frac{\mathrm{d}\boldsymbol{F}}{\mathrm{d}\boldsymbol{U}} = \begin{bmatrix} i\tilde{\nu}[n] & \hat{Z} & \hat{Y} & i[n]\boldsymbol{X} \\ -\hat{Z} & i\tilde{\nu}[n] & -\hat{X} & i[n]\boldsymbol{Y} \\ \hat{Y} & \hat{X} & i\tilde{\nu}[n] & i[n]\boldsymbol{Z} \\ \boldsymbol{1} & \boldsymbol{0} & \boldsymbol{0} & 0 \\ \boldsymbol{0} & \boldsymbol{1} & \boldsymbol{0} & 0 \\ \boldsymbol{0} & \boldsymbol{0} & \boldsymbol{1} & 0 \end{bmatrix} \tag{72}$$

where $\boldsymbol{1}$ and $\boldsymbol{0}$ are $(2N + 1)$ row vectors of ones and zeros, respectively. We observe that there are $6(N + 1)$ equations and only $6N + 4$ unknowns, so that the problem is overdetermined for a fixed N. This is resolved by employing least squares.

Unless a better initial guess is available, we use the solution for asymptotically large Z, which coincides with the solution for an axisymmetric body as discussed in Ref. 10. This solution has constant Z and simple harmonic X and Y. The corresponding coefficients for intermediate-axis torque, $\boldsymbol{\theta} = [0, 1, 0]^T$, are

$$\boldsymbol{X} = i[1/Z(0) - Y(0) - iX(0), 0, -1/Z(0) - Y(0) + iX(0)]^T/2$$

$$\boldsymbol{Y} = -[1/Z(0) - Y(0) - iX(0), -2/Z(0), 1/Z(0) - Y(0) + iX(0)]^T/2$$

$$\boldsymbol{Z} = [0, Z(0), 0]^T$$

$$\tilde{\nu} = Z(0) \tag{73}$$

and for the minor-axis torque case, $\boldsymbol{\theta} = [1, 0, 0]^T$,

$$\boldsymbol{X} = [1/Z(0) + X(0) - i\,Y(0), -2/Z(0), 1/Z(0) + X(0) + iY(0)]^T/2$$

$$\boldsymbol{Y} = i[1/Z(0) + X(0) - iY(0), 0, -1/Z(0) + X(0) + iY(0)]^T/2$$

$$\boldsymbol{Z} = [0, Z(0), 0]^T$$

$$\tilde{\nu} = Z(0) \tag{74}$$

When the applied torque is very large, Newton's method does not converge with the guess as given. This problem is circumvented by replacing the zeros in the initial guess for $\boldsymbol{Z}$ [Eqs. (73) and (74)] with a small nonzero number such as $-Z(0)/100$.

For the kinematics problem, Eqs. (64) and (65), we define a truncated state vector

$$\boldsymbol{U} = [\boldsymbol{u}^T, \boldsymbol{v}^T, s]^T \tag{75}$$

where $\boldsymbol{u}$ and $\boldsymbol{v}$ denote column vectors of the $(2N + 1)$ coefficients, stacked as in Eq. (67):

$$\boldsymbol{F}(\boldsymbol{U}) = \begin{bmatrix} (2sI - A)\begin{bmatrix}\boldsymbol{u} \\ \boldsymbol{v}\end{bmatrix} \\ u_0 - 1 \end{bmatrix} \tag{76}$$

where

$$A = \begin{bmatrix} \hat{\omega}_z - \nu[n] & -\hat{\bar{\omega}}^{\dagger} \\ -\hat{\omega} & -\hat{\omega}_z - \nu[n] \end{bmatrix} \tag{77}$$

and the matrix denoted with the dagger (†) indicates reverse order in the counter [see Eq. (64)]. The Jacobian, $d\boldsymbol{F}/d\boldsymbol{U}$, is easily obtained from Eq. (76).

We note that Eq. (76) is a standard eigenvalue problem. In Ref. 10 we formulate this problem where the A matrix is banded due to the simple harmonic nature of the transverse angular velocities. A numerical algorithm is given that exploits the banded structure. In the general case, the A matrix in Eq. (77) is full because of the presence of higher harmonics; nevertheless, we could solve Eq. (76) using the techniques of Ref. 10. In this paper we present several alternative methods that are computationally more efficient in the full matrix case.

We begin the kinematic iteration with the following initial guess for $\boldsymbol{u}$ and $\boldsymbol{v}$

$$\boldsymbol{u} = [0 \quad 1 \quad 0]^T, \qquad \boldsymbol{v} = [0 \quad 0 \quad 0]^T \tag{78}$$

The initial guess for the eigenvalue s is taken to be $\omega_{z0}/2$, consistent with the small-torque approximation.[10]

Perturbation Method

The perturbation method consists of iteratively executing a particular arrangement of Eqs. (60–65) to determine the Fourier coefficients and the frequencies. For the dynamics problem (60–63), it is convenient to combine X and Y into a single complex number ζ, with corresponding Fourier coefficients ζ_n:

$$\zeta = X + iY \tag{79}$$

Initially ζ_n and Z_n are set to zero. Next, we implement the following equations in the order given:

$$Z_0 \leftarrow Z_0 + Z(0) - \sum_m Z_m \tag{80}$$

$$\zeta_0 \leftarrow \zeta_0 + \left(i\mu - \sum_m Z_m \zeta_{-m} \right) \Big/ Z_0 \tag{81}$$

$$\zeta_1 \leftarrow \zeta_1 + \zeta(0) - \sum_m \zeta_m \tag{82}$$

$$P_n \leftarrow \sum_m Z_m \zeta_{n-m} \tag{83}$$

$$\tilde{\nu} \leftarrow P_1/\zeta_1 \tag{84}$$

$$Q_n \leftarrow \sum_m \zeta_m \zeta_{n-m} \tag{85}$$

$$Z_n \leftarrow (1/4n\tilde{\nu})(Q_n - \bar{Q}_{-n}), \qquad n \neq 0 \tag{86}$$

$$\zeta_n \leftarrow [1/(n\tilde{\nu} - Z_0)](-i\mu\delta_{n0} - Z_0\zeta_n + P_n), \qquad n \neq 1 \tag{87}$$

where $\mu = \mu_x + i\mu_y$. At the end of each iteration, we check if the magnitude of the tail-end Fourier coefficients and the changes in the coefficients fall within the specified error bound. The iteration stops when the convergence criteria are met.

A similar procedure is used for kinematic equations (64) and (65). We begin this process with an initial guess of $u_n = \delta_{n0}$ and $v_n = 0$ and precomputed dynamics coefficients. The iteration equations are

$$s \leftarrow \frac{1}{2} \sum_m (\omega_{zm} u_{-m} - \bar{\omega}_{-m} v_{-m}) \tag{88}$$

$$u_n \leftarrow \frac{1}{2(s + n\nu - \omega_{z0}/2)} \times \left[-\omega_{z0} u_n + \sum_m (\omega_{zm} u_{n-m} - \bar{\omega}_{-m} v_{n-m}) \right], \qquad n \neq 0 \tag{89}$$

$$v_n \leftarrow \frac{-1}{2(s + n\nu + \omega_{z0}/2)} \times \left[-\omega_{z0} v_n + \sum_m (\omega_m u_{n-m} + \omega_{zm} v_{n-m}) \right] \tag{90}$$

which are repeated until the accuracy criteria are met.

The solutions for u_n and v_n given in both the Newton and perturbation methods generate a particular solution for α_q and β_q. We use symmetry to get a second solution.

Numerical Tests

To determine the relative merits of the three solution methods, we conduct numerical experiments. The one-period numerical integration method applies to any torque. On the other hand (for cases with very large torque), Newton's method and the perturbation method sometimes diverge. The total number of floating point operations (FLOPs) to achieve a fixed accuracy is used as the criteria for rating the methods.

We use the one-period integration method to specify a yardstick for comparing FLOPs. The unit measure includes the number of FLOPs to solve for the period using Eq. (33), the number of FLOPs to integrate the governing differential equations (5–7) and (40) and (41) using an adaptive Runge–Kutta fourth/fifth-order integrator, and the number of FLOPs to convert the discrete time histories to Fourier coefficients via FFT. Henceforth we refer to this measure of FLOPs with respect to the one-period method as unity.

We consider Galileo-like spacecraft maneuvers[21] to test the algorithms. The principal moments of inertia are

$$I_x = 2761 \text{ kg} \cdot \text{m}^2, \qquad I_y = 3012 \text{ kg} \cdot \text{m}^2, \qquad I_z = 4627 \text{ kg} \cdot \text{m}^2 \tag{91}$$

which correspond to the nondimensional parameters, κ_x, κ_y, and κ_z

$$\kappa_x = 5.455, \qquad \kappa_y = 5.614, \qquad \kappa_z = 1.661 \tag{92}$$

The following angular velocity initial conditions are chosen:

$$\omega_x(0) = \omega_y(0) = X(0) = Y(0) = 0 \tag{93}$$

and

$$\omega_z(0) = 0.33 \text{ rad/s} \tag{94}$$

Intermediate-Axis Torque Case

When torque is applied along the intermediate axis, $\boldsymbol{\theta} = [0, 1, 0]^T$, the angular velocity vector is periodic for (essentially) any initial condition and torque magnitude. For the initial conditions specified, we find that Newton's method always converges. However, the perturbation method diverges in the kinematic solution where $M_y > 115 \text{ N} \cdot \text{m}$ [$Z(0) < 2.41$] and in both (dynamic and kinematic) solutions when $M_y > 490 \text{ N} \cdot \text{m}$ [$Z(0) < 1.17$].

To demonstrate that only a few Fourier terms are needed when the torque is small, we select

$$M_y = 10 \text{ N} \cdot \text{m}, \qquad [Z(0) = 8.17] \tag{95}$$

Here, all three methods converge for both the angular velocities and the kinematic parameters, and the maximum nutation angle is quite small, just over 0.09 rad or 5 deg (Fig. 4). Figure 5 shows the spectra

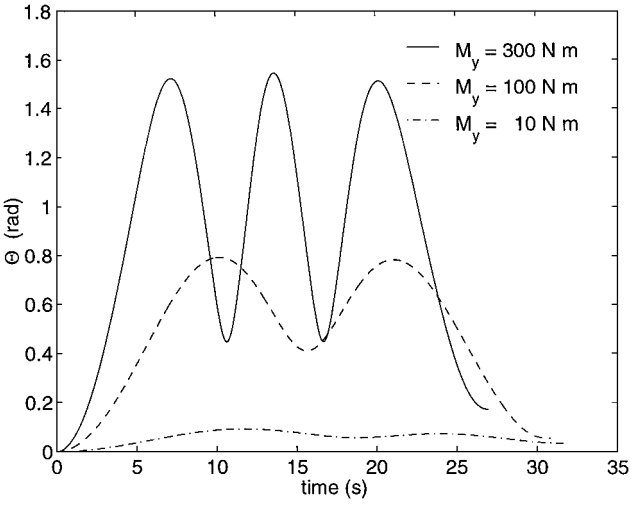

Fig. 4 Nutation angle $\Theta(t)$ for $M_y = [10, 100, 300]$ N ·m.

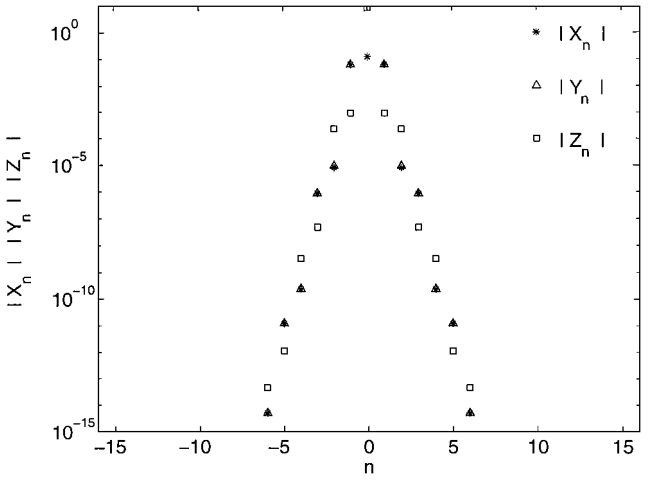

Fig. 5 Spectral plot: angular velocity X_n, Y_n, and Z_n for $M_y = 10$ N ·m.

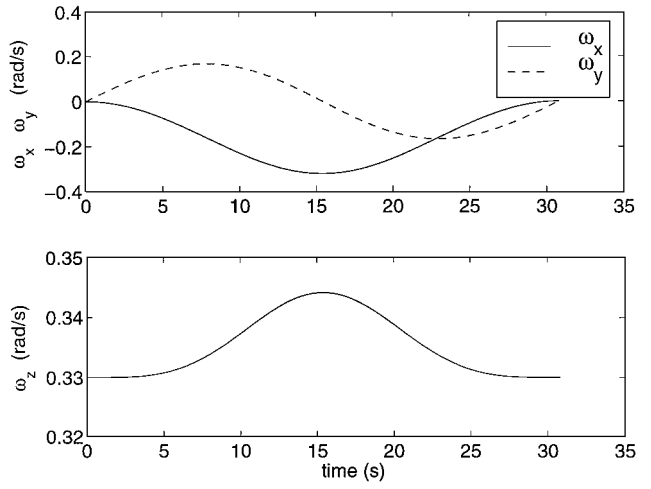

Fig. 6 Angular velocity $\omega_x(t)$, $\omega_y(t)$, and $\omega_z(t)$ for $M_y = 100$ N ·m.

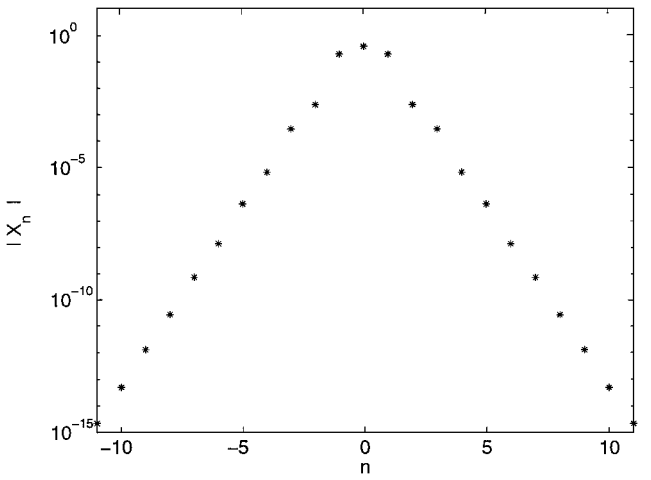

Fig. 7 Spectral plot: angular velocity X_n for $M_y = 100$ N ·m.

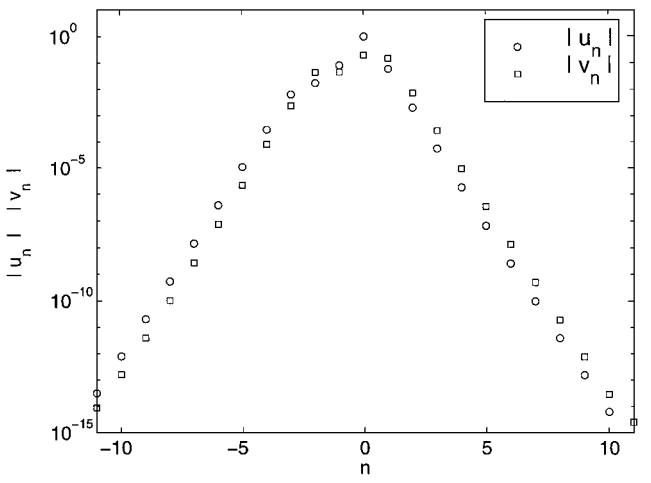

Fig. 8 Spectral plot: kinematic parameters u_n and v_n for $M_y = 100$ N ·m.

for the nondimensional angular velocity coefficients X_n, Y_n, and Z_n. We notice that the largest Z_n coefficient (Z_0) is at least four orders of magnitude greater than the other terms, confirming the appropriateness of the constant spin assumption in the small-torque case.[10] The largest X_n and Y_n coefficients correspond to simple harmonics ($n = -1, 0, 1$), with all other terms being at least four orders of magnitude smaller. For an error bound of 10^{-6}, Newton's method uses 1.1 times the number of unit FLOPs whereas the perturbation method uses only 3% of the unit FLOPs. The success of the perturbation method is due in large part to the rapid decay of the Fourier coefficients (Fig. 5).

The moderately large torque,

$$M_y = 100\ \text{N}\cdot\text{m}, \qquad [Z(0) = 2.58] \tag{96}$$

corresponds to the nearly axisymmetric case presented in Ref. 10. Time histories of the angular velocities, ω_x, ω_y, and ω_z are plotted in Fig. 6. The spin rate ω_z is not constant (as assumed in Ref. 10), but periodic with a 10% fluctuation in amplitude. The corresponding nutation angle (Fig. 4) achieves a maximum value of 0.79 rad (just over 45 deg). In this case, Newton's method uses 2.7 unit FLOPs, whereas the perturbation method uses only 17% of the unit FLOPs. Figures 7 and 8 show the spectra of the nondimensional angular velocity coefficients X_n and the kinematic parameters u_n and v_n. (The spectra of Y_n and Z_n are similar.) From Fig. 8, we see that we need just as many Fourier terms for the kinematic parameters as for the angular velocities regardless of the tolerance chosen. The number of terms required is proportional to the logarithm of the tolerance.

We select a large torque,

$$M_y = 300\ \text{N}\cdot\text{m}, \qquad [Z(0) = 1.49] \tag{97}$$

to demonstrate the theory for an extreme case where the spacecraft nutation angle Θ is about 90 deg (Fig. 4). In this case, Newton's method uses 2.2 unit FLOPs. Although the perturbation method converges for the dynamics problem, it diverges for the kinematic problem. Further tests show that even when the exact Fourier coefficients are given as the initial guess, the perturbation method diverges, and so the method is locally unstable.

Minor-Axis Torque Case

When torque is applied along the minor axis, $\boldsymbol{\theta} = [1, 0, 0]^T$, the motion is periodic when $M_x < 215$ N · m [$Z(0) > 1.66$]. Newton iteration and the perturbation expansion for the dynamics both converge over this entire range. However, the perturbation series diverges for the kinematics at torques of $M_x > 85$ N · m [$Z(0) < 2.64$].

For the small torque,

$$M_x = 10\ \text{N}\cdot\text{m}, \qquad [Z(0) = 7.71] \tag{98}$$

corresponding to the circle in Fig. 2, all three methods converge for both the angular velocities and the kinematic parameters. The maximum nutation angle is quite small, just under 0.104 rad or 6 deg (Fig. 3). Newton's method uses 1.7 unit FLOPs whereas the perturbation method uses only 3%.

The large torque,

$$M_x = 200\ \text{N}\cdot\text{m}, \qquad [Z(0) = 1.72] \tag{99}$$

corresponds to the × in Fig. 2, near the upper boundary. The angular velocity time histories and spectra are similar to the results of Figs. 6 and 7. The nutation angle, shown in Fig. 3, achieves a maximum of about 1.7 rad (97 deg) at 22 s. In this case, Newton's method

Table 1 Summary of results for test cases

	Intermediate-axis torque M_y, N·m			Minor-axis torque M_x, N·m	
Method	10	100	300	10	200
One-period integration, unit FLOPs	1	1	1	1	1
Newton's method, unit FLOPs	1.1	2.7	2.2	1.7	17
Perturbation method, unit FLOPs	0.03	0.17	Div[a]	0.03	Div[a]
Number of harmonics, 10^{-6} error bound	4	5	8	4	8

[a]Algorithm diverges.

uses 17 times the number of unit FLOPs. The perturbation method converges for the dynamics, but diverges for the kinematic solution.

Discussion

In Table 1, we present a summary of the results for the five test cases. For small to moderate torques, the perturbation method is by far the most efficient. However, it diverges when the torque is excessive. Newton's method, although fairly robust, always uses more FLOPs than the other two methods to achieve the (10^{-6}) error bound specified. The efficiency of the one-period integration method could be improved by using a higher-order method, particularly when high accuracy is required.

It is apparent from these results that relatively few harmonics are needed even for high accuracy. Once the Fourier coefficients have been determined, the solution can be continued through any number of periods with negligible additional cost (FLOPs). Of course any error in the determination of the fundamental frequencies will produce an accumulated phase error, but no accumulation of amplitude error can occur. In contrast, if solutions are obtained by pure numerical integration, both amplitude and phase errors will generally accumulate over time, and the cost will be proportional to the number of periods simulated. To ensure a given error bound in the Nth period, an even tighter integration tolerance must be imposed throughout the simulation than would be needed for just the first period. Therefore, the cost (in unit FLOPs) for a fixed terminal error would be greater than N.

Conclusions

Floquet techniques are used to analyze the motion of an asymmetric rigid body with principal axis torque. For typical spacecraft torque levels, only a few Fourier terms are needed. Of the three methods presented, the one-period integration is the most robust. It is guaranteed to work whenever the motion of the angular velocity vector is periodic. Whereas the perturbation method diverges for large torque, for small to moderate torque it uses fewer FLOPs than the other methods to achieve a specified accuracy. These methods are more efficient than brute force numerical integration and may find application in onboard computations for spacecraft maneuvers, where speed, accuracy, and memory place severe constraints on numerical algorithms.

Acknowledgments

This research is supported in part by NASA Headquarters under Grant NGT5-50110 (NASA program official Dolores Holland) and by the Purdue Forever Fellowship.

References

[1]Leimanis, E., *The General Problem of the Motion of Coupled Rigid Bodies About a Fixed Point*, Springer–Verlag, New York, 1965, Chap. 2.

[2]Larson, V., and Likins, P. W., "Closed-Form Solutions for the State Equation for Dual-Spin and Spinning Spacecraft," *Journal of the Astronautical Sciences*, Vol. 21, No. 5–6, 1974, pp. 244–251.

[3]Kraige, L. G., and Junkins, J. L., "Perturbation Formulations for Satellite Attitude Dynamics," *Celestial Mechanics*, Vol. 13, No. 1, 1976, pp. 39–64.

[4]Kraige, L. G., and Skaar, S. B., "A Variation of Parameters Approach to the Arbitrarily Torqued, Asymmetric Rigid Body Problem," *Journal of the Astronautical Sciences*, Vol. 25, No. 3, 1977, pp. 207–226.

[5]Kane, T. R., and Levinson, D. A., "Approximate Solution of Differential Equations Governing the Orientation of a Rigid Body in a Reference Frame," *Journal of Applied Mechanics*, Vol. 54, No. 1, 1987, pp. 232–234.

[6]Longuski, J. M., "Real Solutions for the Attitude Motion of a Self-Excited Rigid Body," *Acta Astronautica*, Vol. 25, No. 3, 1991, pp. 131–140.

[7]Or, A. C., "Injection Errors of a Rapidly Spinning Spacecraft with Asymmetries and Imbalances," *Journal of the Astronautical Sciences*, Vol. 40, No. 3, 1992, pp. 419–427.

[8]Longuski, J. M., and Tsiotras, P., "Analytic Solution of the Large Angle Problem in Rigid Body Attitude Dynamics," *Journal of the Astronautical Sciences*, Vol. 43, No. 1, 1995, pp. 25–46.

[9]Randall, L. A., Longuski, J. M., and Beck, R. A., "Complex Analytic Solutions for a Spinning Rigid Body Subject to Constant Transverse Torques," American Astronautical Society, Paper 95-373, Aug. 1995.

[10]Gick, R. A., Williams, M. H., and Longuski, J. M., "Floquet Approximation for a Nearly Axisymmetric Rigid Body with Constant Transverse Torque," *Journal of Guidance, Control, and Dynamics*, Vol. 22, No. 5, 1999, pp. 658–663.

[11]Meirovitch, L., *Methods of Analytical Dynamics*, McGraw–Hill, New York, 1970, pp. 264–280.

[12]Nayfeh, A. H., and Balachandran, B., *Applied Nonlinear Dynamics*, Wiley, New York, 1995, pp. 158–172.

[13]Calico, R. A., and Wiesel, W. E., "Control of Time-Periodic Systems," *Journal of Guidance, Control, and Dynamics*, Vol. 7, No. 6, 1984, pp. 671–676.

[14]Mingori, D. L., "Effects of Energy Dissipation on the Attitude Stability of Dual-Spin Satellites," *AIAA Journal*, Vol. 7, No. 1, 1969, pp. 20–27.

[15]Noah, S. T., and Hopkins, G. R., "A Generalized Hill's Method for Stability Analysis of Parametrically Excited Dynamic Systems," *Journal of Applied Mechanics*, Vol. 49, No. 1, 1982, pp. 217–223.

[16]Livneh, R., and Wie, B., "New Results for an Asymmetric Rigid Body with Constant Body-Fixed Torques," *Journal of Guidance, Control, and Dynamics*, Vol. 20, No. 2, 1997, pp. 873–881.

[17]Greenwood, D. T., *Principles of Dynamics*, Prentice–Hall, Englewood Cliffs, NJ, 1988, pp. 119–122.

[18]Shuster, M. D., "A Survey of Attitude Representations," *Journal of the Astronautical Sciences*, Vol. 41, No. 4, 1993, pp. 439–518.

[19]Goldstein, H., *Classical Mechanics*, Addison–Wesley, Reading, MA, 1980, pp. 148–158.

[20]Meirovitch, L., *Introduction to Dynamics and Control*, Wiley, New York, 1985, pp. 183, 184.

[21]Longuski, J. M., Kia, T., and Breckenridge, W. G., "Annihilation of Angular Momentum Bias During Thrusting and Spinning-Up Maneuvers," *Journal of the Astronautical Sciences*, Vol. 37, No. 4, 1989, pp. 433–450.